Effect of Compression Ratio on Cycle-by-Cycle Variations in a Natural Gas Direct Injection Engine

ARTICLE *in* PROCEEDINGS OF THE INSTITUTION OF MECHANICAL ENGINEERS PART D JOURNAL OF AUTOMOBILE ENGINEERING · MARCH 2013

Impact Factor: 0.83 · DOI: 10.1021/ef900651p

Energy Fuels **2009,** *23,* 5357–5366 · DOI:10.1021/ef900651p
Published on Web 09/16/2009

energy&fuels
article

Effect of Compression Ratio on Cycle-by-Cycle Variations in a Natural Gas Direct Injection Engine

Jianjun Zheng, Zuohua Huang,* Jinhua Wang, Bin Wang, Dezhong Ning, and Yingjia Zhang

State Key Laboratory of Multiphase Flow in Power Engineering, Xi'an Jiaotong University, Xi'an, People's Republic of China

Received June 27, 2009. Revised Manuscript Received August 31, 2009

Cycle-by-cycle variations of a natural gas direct-injection spark ignition engine at different compression ratios were investigated. The results show that the lean burn limit of the natural-gas direct injection engine can be extended to a larger overall excess air ratio compared with that of the homogeneous charge natural gas engine. The coefficient of variations (CoV) of indicated mean effective pressure decreases with the increase of compression ratio. However, CoV of indicated mean effective pressure is increased at high engine load when compression ratio is larger than 12. The cycle-by-cycle variations are more clearly demonstrated in CoV of indicated mean effective pressure rather than in CoV of cylinder peak pressure. Average values of flame development duration, main combustion duration, and total combustion duration are decreased and combustion is improved with increasing compression ratio. This is the reason for decreasing cycle-by-cycle variations in the natural gas direct-injection engine. Better interdependence exists between the indicated mean effective pressure and the flame development duration, as well as between the indicated mean effective pressure and late combustion duration. Cycle-by-cycle variations of the natural gas direct-injection engine are resulted from cycle-by-cycle variations in flame development duration and late combustion duration. This shows some difference to that of homogeneous charge natural gas engine, where cycle-by-cycle variations are mainly influenced by the variations in early flame development stage.

1. Introduction

With increasing concern about fuel shortage and air pollution control, research on improving engine fuel economy and reducing exhaust emissions has become the major topic in combustion and engine studies. Because of limited reserves of crude oil, the development of alternative-fuel engines has attracted more attention in the engine community. Alternative fuels usually are clean fuels compared with traditional diesel fuel and gasoline fuel in the engine combustion process. The introduction of these alternative fuels is beneficial to slowing down the fuel shortage and reducing engine exhaust emissions.

Natural gas is thought to be one of the most promising alternatives to traditional vehicle fuels for engines since it has cleaner combustion characteristics and plentiful reserves. Natural gas is widely used in taxis and city buses all over the world, and the natural-gas-fueled engine has been realized in both the spark-ignition engine and the compression-ignition engine. Furthermore, its high-octane value and good antiknock property permits high compression ratio leading, of course, to higher thermal efficiency under high load condition. Previous studies showed low emissions by using natural gas. Engines fuelled with natural gas emit less carbon-monoxide and nonmethane hydrocarbons compared with gasoline engines.[1,2]

Nowadays, there are mainly two kinds of operating mode for engines fueled with natural gas in actual applications (or during routine operation). In the first operating mode, the homogeneous natural gas is ignited by pilot injection of the diesel fuel before the top-dead center. This needs two separate fueling systems and makes the system complicated. Meanwhile, hydrocarbon (HC) emissions still remain high at light loads. In the second mode, the homogeneous mixture of natural gas and air is ignited by a spark plug as in the traditional homogeneous gasoline spark-ignited engine. As natural gas occupies some fraction of intake charge, it has the disadvantage of low volumetric efficiency, and this decreases the amount of fresh air in the cylinder, leading to decreased power output compared with that of a gasoline engine. The homogeneous charge combustion makes it difficult to burn the lean mixture. These engines have a lower thermal efficiency because of engine knock restriction and unavoidable throttling at the intake at partial load.[3] So-called homogeneous lean combustion engines have appeared. These can realize a higher thermal efficiency owing to the lower pumping loss, the lower heat loss, and the increase in the specific heat ratio, at the expense of the moderately higher NO_x emissions due to the ineffectiveness of the existing catalyst. The large cycle-by-cycle variation, however, restricts the lean operation limit of this type of homogeneous mixture engines.[4−8]

*To whom correspondence should be addressed. Telephone: +86 29 82665075. Fax: +86 29 82668789. E-mail: zhhuang@mail.xjtu.edu.cn.

(1) Weaver, C. S. *Natural Gas Vehicles — A Review of the State of the Art*, SAE Paper 892133; Society of Automotive Engineers: Warrendale, PA, 1989.

(2) Rousseau, S.; Lemoult, B.; Tazerout, M. *Proc. Inst. Mech. Eng., Part D* **1999**, *213* (5), 481–489.

(3) Yamamoto, Y.; Sato, K.; Matsumoto, S. *Study of Combustion Characteristics of Compressed Natural Gas As Automotive Fuel*, SAE Paper 940761; Society of Automotive Engineers: Warrendale, PA, 1994.

(4) Ben, L.; Dacros, N. R.; Truquet, R.; Charnay, G. *Influence of Air/Fuel Ratio on Cyclic Variation and Exhaust Emission in Natural Gas SI Engine*, SAE Paper 992901; Society of Automotive Engineers: Warrendale, PA, 1999.

(5) Hassaneen, A. E.; Varde, K. S.; Bawady, A. H.; Morgan, A. A. *A Study of the Flame Development and Rapid Burn Durations in a Lean-Burn Fuel Injected Natural Gas S.I. Engine*, SAE Paper 981384; Society of Automotive Engineers: Warrendale, PA, 1998.

In recent years, a gasoline direct-injection (GDI) engine has entered into the stage of production for modern two- and four-stroke petrol engines. The major advantages of a GDI engine are the increase in the fuel efficiency. The charge stratification formed by fuel injection and turbulence in the combustion chamber permits extremely lean combustion without high cycle-by-cycle variations, leading to a high combustion efficiency and low emissions at low load.[9−11] In addition, there is no throttling loss in some GDI engines, which greatly improves the volumetric and thermal efficiencies in engines without a throttle valve. Moreover, the end gas mixture near the cylinder wall is very lean, reducing the occurrence of knocking, and this allows utilization of an increased compression ratio to improve engine performance and thermal efficiency.

Direct injection natural gas can be utilized to avoid the loss in volumetric efficiency, as natural gas is directly injected into the cylinder. It is flexible in mixture preparation because of forming a stratified mixture in the cylinder at low loads and improving the fuel economy. The ability to increase the compression ratio can improve the engine performance. In addition, natural gas direct-injection combustion can avoid smoke emission from gasoline direct-injection combustion.[12−15] Some previous studies were conducted on natural gas direct-injection combustion by using a rapid compression machine and/or engines.[15−25]

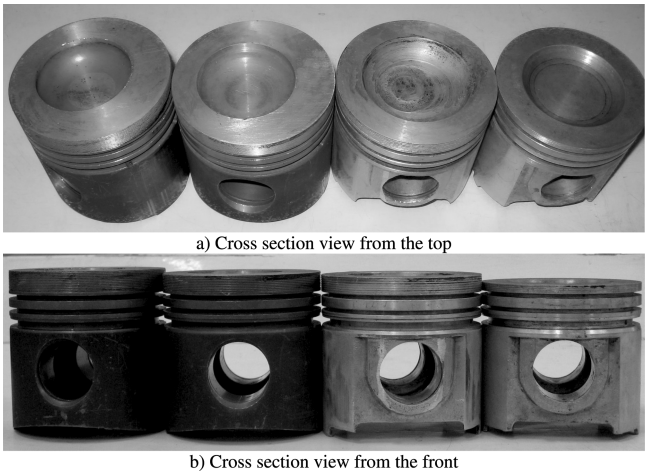

a) Cross section view from the top

b) Cross section view from the front

Figure 1. Pistons at different compression ratios (compression ratios of 14, 12, 10, and 8, from left to right).

Table 1. Engine Specifications

number of cylinder	1
bore × stroke (mm)	100 × 115
length of connecting rod (mm)	190
compression ratio	8, 10, 12, 14
combustion chamber	bowl-in-shape
displacement (L)	0.903
ignition source	spark plug
injection pressure (MPa)	8
inlet valve opening	11°CA BTDC
inlet valve closure	49°CA ABDC
exhaust valve opening	52°CA BBDC
exhaust valve closure	8°CA ATDC

The cycle-by-cycle variations exist in spark ignition engines, and this phenomenon will become more severe at lean burn or highly diluted mixtures such as high EGR ratio.[26] Many studies were conducted on the cycle-by-cycle variations of spark ignition engines; and the studies revealed that the variations in the early combustion stage mainly determined the cycle-by-cycle variations of engines, and any approaches that increase the burning velocity of the mixtures will lead to the reduction of the cycle-by-cycle variations of engines.[26−32]

(6) Ramesh, A.; Corre, O.; Tazerout, M. Experimental investigation on cycle by cycle variations in a natural gas fulled spark ignition engine. In *Proceedings of the Second International SAE India Mobility Conference*, Chennai, India, Jan. 10−12, 2002; SAE International, Univerdale, Pennsylvania, 2002; pp 145−152.
(7) Choa, H. M.; He, B. Q. *Energy Convers. Manage.* **2007**, *48* (2), 608–618.
(8) Corbo, P.; Gambino, M.; Iannaccone, S.; Unich, A. *Comparison between Lean-Burn and Stoichiometric Technologies for CNG Heavy-Duty Engines*, SAE Paper 950057; Society of Automotive Engineers: Warrendale, PA, 1995.
(9) Brehob, D. D.; Stein, R. A.; Haghgooie, M. *Stratified-Charge Engine Fuel Economy and Emission Characteristics*, SAE Paper 982704; Society of Automotive Engineers: Warrendale, PA, 1998.
(10) Kano, M.; Saito, K.; Basaki, M. *Emissions and Fuel Economy of a 1998 Toyota with a Direct Injection Spark Ignition Engine*, SAE Paper 981462; Society of Automotive Engineers: Warrendale, PA, 1998.
(11) Iwamoto, Y.; Noma, K.; Nakayama, O.; Yamauchi, T.; Ando, H. *Development of Gasoline Direct Injection Engine*, SAE Paper 970541; Society of Automotive Engineers: Warrendale, PA, 1997.
(12) Willi, M. L.; Richards, B. G. *J. Eng. Gas. Turbines Power* **1995**, *117* (4), 799–803.
(13) Meyers, D. P.; Bourn, G. D.; Hedrick, J. C.; Kubesh, J. T. *Evaluation of Six Natural Gas Combustion Systems for LNG Locomotive Applications*, SAE Paper 972967; Society of Automotive Engineers: Warrendale, PA, 1997.
(14) Huang, Z. H.; Wang, J. H.; Liu, B.; Zeng, K.; Yu, J. R.; Jiang, D. M. *Energy Fuels* **2006**, *20* (2), 540–546.
(15) Zeng, K.; Huang, Z. H.; Liu, B.; Liu, L. X.; Jiang, D. M.; Ren, Y.; Wang, J. H. *Appl. Therm. Eng.* **2006**, *26* (8−9), 806–813.
(16) Huang, Z. H.; Liu, L. X.; Jiang, D. M.; Ren, Y.; Liu, B.; Zeng, K.; Wang, Q. *Proc. Inst. Mech. Eng., Part D* **2008**, *222* (9), 1657–1667.
(17) Honjo, F.; Miura, A.; Nakamura, A.; Tsuchiya, T. CNG in-cylinder direct injection engine system. In *Proceedings of the JSAE Annual Congress*; Society of Automotive Engineers of Japan: Tokyo, 2004; Vol. 118 (04), pp 13−16 .
(18) Yuichi, G. *JSME Int. J. B: Fluids Therm. Eng.* **1999**, *42* (2), 268–274.
(19) Hill, P. G.; Douville, B. *J. Eng. Gas. Turbines Power* **2000**, *122* (1), 141–149.
(20) Douville, B.; Ouellette, P.; Touchette, A.; Ursu, B. *SAE Trans.* **1998**, *107* (3), 1727–1735.
(21) Huang, Z. H.; Shiga, S.; Ueda, T.; Jingu, N.; Nakamura, H.; Ishima, T.; Obokata, T.; Tsue, M.; Kono, M. *JSME Int. J. B: Fluids Therm. Eng.* **2002**, *45* (4), 891–900.
(22) Huang, Z.; Shiga, S.; Ueda, T.; Nakamura, H.; Ishima, T.; Obokata, T.; Tsue, M.; Kono, M. *Proc. Inst. Mech. Eng., Part D* **2003**, *217* (5), 393–401.
(23) Huang, Z.; Shiga, S.; Ueda, T. *J. Eng. Gas. Turbines Power* **2003**, *125* (3), 783–790.
(24) Huang, Z.; Shiga, S.; Ueda, T.; Nakamura, H.; Ishima, T.; Obokata, T.; Tsue, M.; Kono, M. *Proc. Inst. Mech. Eng., Part D* **2003**, *217* (1), 53–62.
(25) Zheng, J. J.; Wang, J. H.; Wang, B.; Huang, Z. H. *Proc. Inst. Mech. Eng., Part D* **2009**, *223* (1), 85–98.
(26) Heywood, J. B. *Internal Combustion Engine Fundamentals*; McGraw-Hill: New York, 1988.
(27) Kalghatgl, G. T. *Spark Ignition, Early Flame Development and Cyclic Variation in I.C. Engines*, SAE Paper 870163; Society of Automotive Engineers: Warrendale, PA, 1987.
(28) Keck, J. C.; Heywood, J. B.; Noske, G. *Early Flame Development and Burning Rates in Spark Ignition Engines and Their Cyclic Variability*, SAE Paper 870164; Society of Automotive Engineers: Warrendale, PA, 1987.
(29) Bates, S. C. *Flame Imaging Studies of Cycle-by-Cycle Combustion Variation in a SI Four-Stroke Engine*, SAE Paper 892086; Society of Automotive Engineers: Warrendale, PA, 1989.
(30) Ishii, K.; Sasaki, T.; Urata, Y.; Yoshida, K.; Ohno, T. *Investigation of Cyclic Variation of Imep under Lean Burn Operation in Spark-Ignition Engine*, SAE Paper 972830; Society of Automotive Engineers: Warrendale, PA, 1997.
(31) Zervas, E. *Appl. Therm. Eng.* **2004**, *24* (14−15), 2073–2081.
(32) Fischer, J.; Velji, A.; Spicher, U. *Investigation of Cycle-to-Cycle Variations of in-Cylinder Processes in Gasoline Direct Injection Engines Operating with Variable Tumble Systems*, SAE Paper 2004−01−0044; Society of Automotive Engineers: Warrendale, PA, 2004.

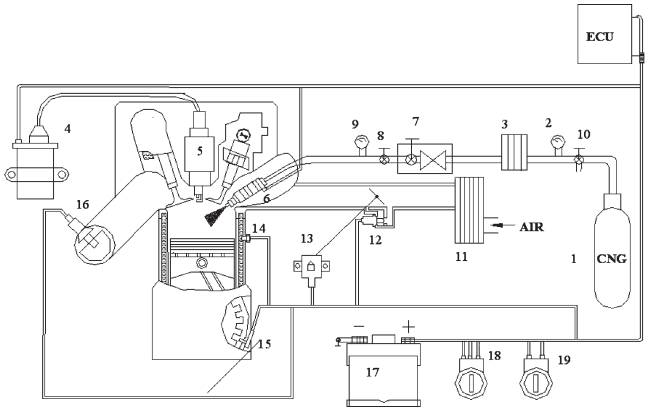

Figure 2. Experimental setup and injector arrangement.

Table 2. Specifications of the Pistons

compression ratio (mm)	piston height (mm)	top land height (mm)	bore of piston cavity (mm)	height of piston cavity (mm)
8	94.12	6.00	69.20	7.30
10	98.44	10.60	68.00	10.78
12	100.00	12.16	59.42	14.20
14	102.40	14.52	58.24	16.84

Das and Watson carried out an experimental investigation on a modified natural gas engine at different compression ratios,[33] and their results showed that increasing the compression ratio combined with cylinder turbulence enhancement allowed burning of lean mixtures without large cyclic variations. If an elevated compression ratio is utilized in the natural gas direct-injection spark ignition engine, it will lead to strong stratified mixture near the spark plug, which will increase the flame development and propagation speed in the early stage of the flame kernel. In addition, the temperature and pressure in cylinder will be increased with increasing compression ratio. Furthermore, the turbulent intensity in cylinder will be enhanced, which will also increase the flame development speed and decrease the cycle-by-cycle variations of the engine. However, too-large compression ratio may lead to an overstratified mixture formed near the spark plug at the ignition timing and/or engine knock and subsequent extra cycle-by-cycle variations for the natural gas direct-injection spark ignition engine. Therefore, it is necessary to determine a compromise compression ratio in the natural gas direct-injection engine to get the stable engine operation and low exhaust emissions. However, few studies on the effect of the compression ratio on cycle-by-cycle variations of the natural gas direct-injection engine were reported. The objective of this study is to experimentally evaluate the effect of compression ratio on cycle-by-cycle variations in a natural gas direct-injection engine and to analyze the cause of cycle-by-cycle variations in the natural gas direct-injection engine. The study can provide the technical guidance to the engine optimization. It needs to be mentioned that, in order to analyze, control, and predict the cycle-by-cycle variations encountered in internal combustion engines, some new analysis methods were proposed, for example wavelet analysis, neural networks, recurrence plots, etc.[34−37] They maybe efficient and fast ways to approximate the parameters that describe the combustion and can be realized in real time in the future. As this will not be

Table 3. Composition of Natural Gas

items	volume percentage
CH_4	96.16
iC_4H_{10}	0.021
nC_5H_{12}	0.005
H_2S	0.0002
C_2H_6	1.096
nC_4H_{10}	0.021
N_2	0.001
H_2O	0.006
C_3H_8	0.136
iC_5H_{12}	0.006

Table 4. Engine Operating Parameters

					Δt_{injd} (ms)			
No.	n_e (rpm)	p_{me} (MPa)	θ_{inj} (CA BTDC)	θ_{ign} (CA BTDC)	CR 8	CR 10	CR 12	CR 14
1	1200	0.14	150	20	14.46	12.42	11.22	10.92
2	1200	0.42	168	24	14.76	14.72	12.82	12.46
3	1200	0.70	180	30	18.26	17.72	16.62	17.06
4	1800	0.14	180	27	15.96	13.82	13.22	12.56
5	1800	0.42	190	32	16.66	14.92	14.19	12.96
6	1800	0.70	210	34	18.26	18.02	15.89	15.46

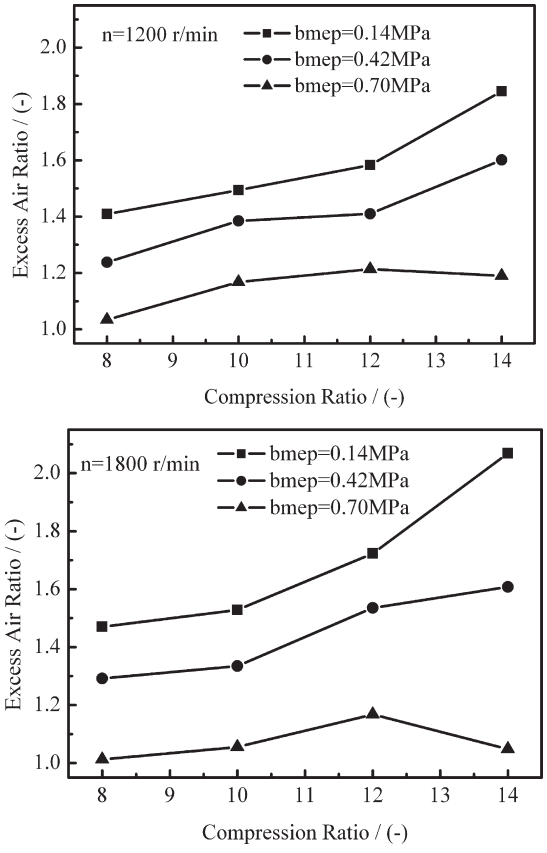

Figure 3. Overall excess air ratio vs compression ratio.

(33) Das, A.; Watson, H. C. *Proc. Inst. Mech. Eng., Part D* **1997**, *211* (5), 361–378.
(34) Sen, A. K.; Litak, G.; Taccani, R.; Radu, R. *Chaos, Solitons Fractals* **2008**, *38* (3), 886–893.
(35) Sen, A. K.; Longwic, R.; Litak, G.; Gorski, K. *Mech. Sys. Signal Process.* **2008**, *22* (2), 362–373.
(36) Longwic, R.; Litak, G.; Sen, A. K. *Z. Naturforschung A* **2009**, *64* (1−2), 96–102.
(37) Muller, R.; Hemberger, H. H.; Baier, K. H. *Meccanica* **2001**, *32* (5), 423–430.

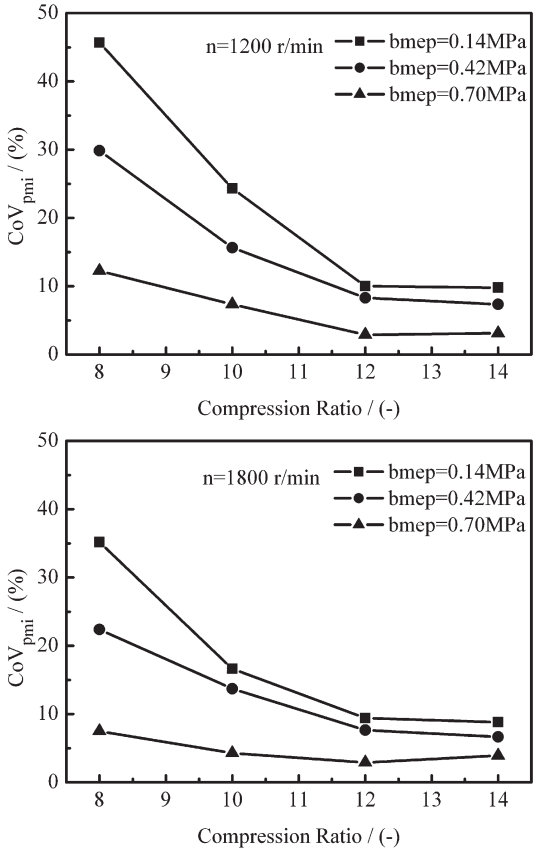

Figure 4. CoV_{pmi} versus compression ratio.

touched upon in this paper, the reader can refer to the literatures above.

2. Experimental Setup

A single-cylinder modified natural gas direct-injection spark ignition engine is used in the study.[14−16] The specifications of the engine are listed in Table 1.

To study the effect of compression ratio on engine cycle-by-cycle variations, four compression ratios by modifying the piston crown were prepared. The images of the modified pistons are shown in Figure 1, and the specifications of the pistons are listed in Table 2.

A production-type of gasoline swirl injector was used in the study. The flow rate of the injector under 8 MPa is 191.8 L/min. In addition to installing the natural gas high-pressure injector, a spark plug was also installed in the combustion chamber as the ignition source, and the experimental setup and injector arrangement is shown in Figure 2.

An electronic control system was used for engine operation and control. Injection timing, spark timing, and injection duration were controlled by the ECU unit and could be regulated in the experiment.

The composition of natural gas used in this experiment is given in Table 3. Natural gas was prepared in advance in a CNG tank and was supplied to the fuel injector through a pressure regulator. Natural gas was injected into cylinder at the constant pressure of 8 MPa, since the gas velocity from the injector nozzle is kept at a constant value of the sonic velocity due to the condition of choke flow during the fuel injection, thus the amount of injected fuel will keep a constant value determined by the injection duration in the study.

The experiments were conducted at 70% WOT and engine speeds of 1200 and 1800 rpm. Six operation modes were conducted to study the effect of compression ratio; the engine

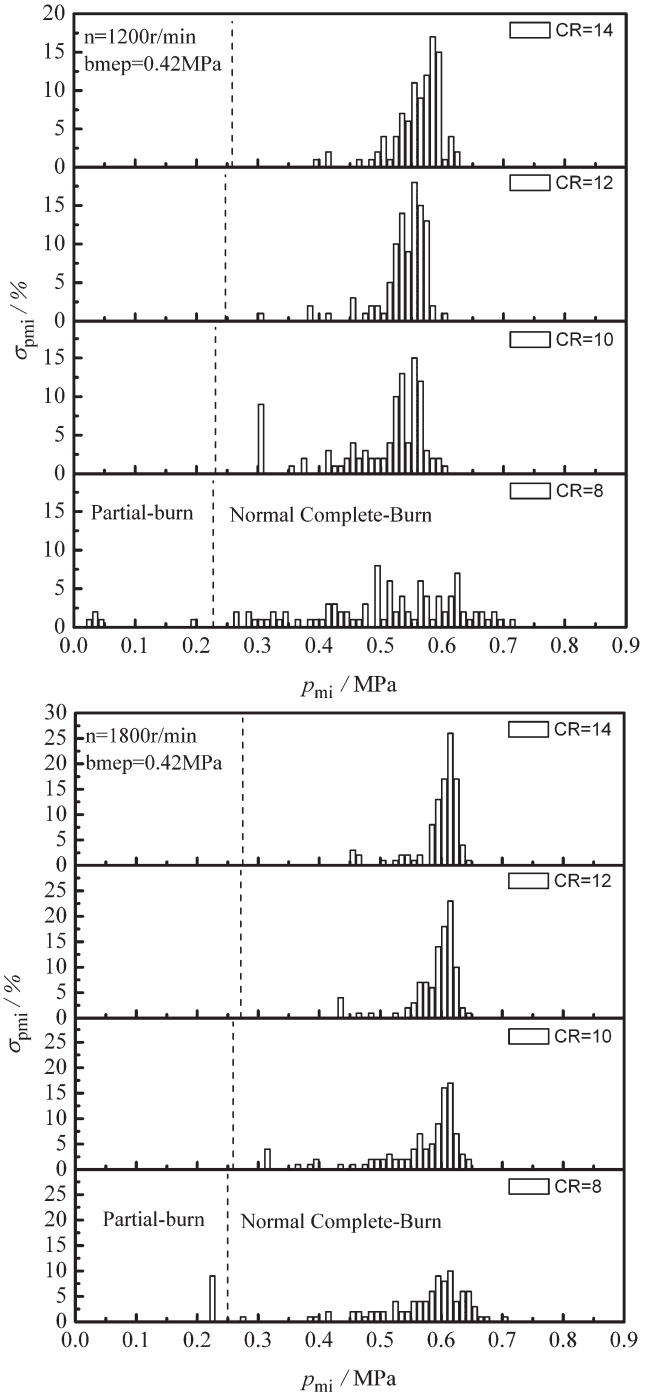

Figure 5. Frequency of p_{mi} distributions at different compression ratios.

operating parameters are listed in Table 4. The experiments were conducted at fixed fuel injection timings and fixed ignition timings for the same mode. Thus, the influence of compression ratio on the cycle-by-cycle variations can be attributed to the influence from variations of compression ratio.

3. Instrumentation and Method of Calculation

An eddy current dynamometer CW40 manufactured by Xiangyi Power Testing Instrument Co. Ltd. is used to measure the engine torque and speed. A Horiba MEXA-720 emission analyzer is used to measure the overall excess air ratios. Cylinder

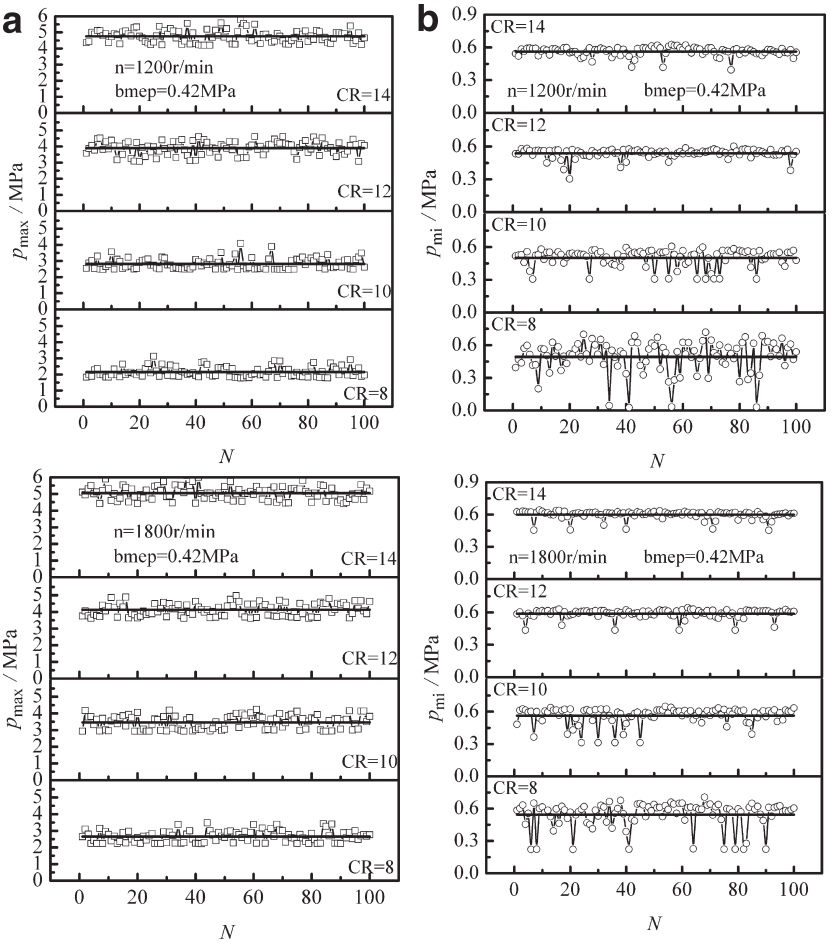

Figure 6. Cyclic variations of p_{max} and p_{mi}.

pressure is recorded by a Kistler piezoelectric transducer (Type 6117BFD17) with the resolution of 10 Pa, and the dynamic TDC is determined by motoring. The crank angle signal was obtained from a Kistler crank angle encoder (Type 2613B) mounted on the main shaft, while the information of pressure and crank angle were recorded by Yokogawa data acquisition system DL750. The signal of the cylinder pressure was acquired for every 0.1 crank angle degree (CAD), and the pressures of 100 consecutive cycles of each stable operating condition are recorded to analyze the cycle-by-cycle variations of the engine.

On the basis of assumed homogeneous cylinder contents and the measured average pressure, a FORTRAN computer data processing program is used to calculate the indicated mean effective pressure (p_{mi}), the maximum pressure (p_{max}), the maximum rate of pressure rise $(dp/d\theta)_{max}$, the corresponding crank angles for maximum pressure, the maximum rate of pressure rise (θ_{pmax} and $\theta_{(dp/d\theta)_{max}}$), the flame development duration ($\Delta\theta_{fd}$), the main combustion duration($\Delta\theta_{md}$), and the total combustion duration ($\Delta\theta_{td}$) for each cycle. The Coefficient of variation (CoV) of indicated mean effective pressure (CoV_{pmi}) and the correlation coefficients between any two variables are calculated by the following formula,[26]

$$\overline{x} = \frac{1}{N}\sum_{i=1}^{N} x_i \tag{1}$$

$$SD_x = \sqrt{\frac{\sum_{i=1}^{N}(x_i - \overline{x})^2}{N}} \tag{2}$$

$$CoV_x = \frac{SD_x}{\overline{x}}100\% \tag{3}$$

$$R(x,y) = \frac{1}{N}\sum_{i=1}^{N}(x_i - \overline{x})(y_i - \overline{y})/(SD_x SD_y) \tag{4}$$

where x_i and y_i represent the specific value of the sample x and y in a combustion cycle. N is the total number of the cycles. $\overline{x}$, SD_x, and CoV_x mean the average value, standard deviation, and the CoV of sample x, respectively. $R(x,y)$ represents the correlation coefficient between samples x and y.

In this paper, the flame-development duration is defined as the interval of crank angle from the ignition start to that of 10% mass fraction burnt; the main-combustion duration is defined as the interval of crank angle from the ignition start to that of 50% mass fraction burnt; the total-combustion duration is defined as the interval of crank angle from the ignition start to that of 90% mass fraction burnt. The mass fraction burnt curve in this paper is determined by the R−W method.[38,39]

(38) Rassweiler, G. M.; Withrow, L. *Motion Pictures of Engine Flames Correlated with Pressure Cards*, SAE Paper 800131; Society of Automotive Engineers: Warrendale, PA, 1980.

(39) Eriksson, L. *Spark Advance for Optimal Efficiency*, SAE Paper 1999−01−0548; Society of Automotive Engineers: Warrendale, PA, 1999.

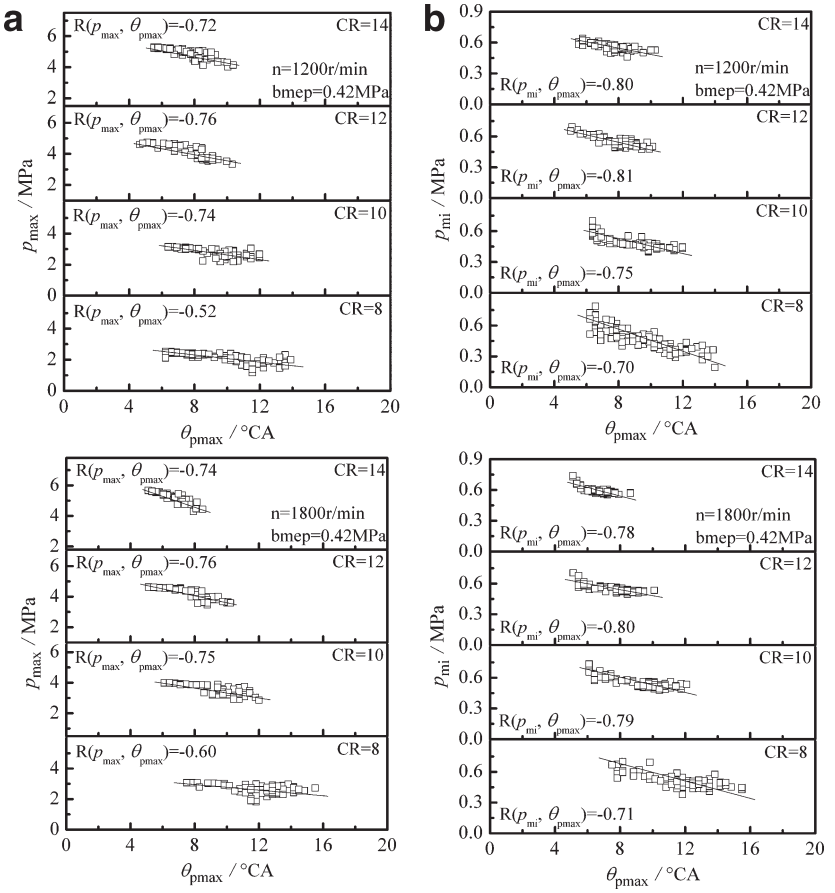

Figure 7. Interdependency between p_{max}, p_{mi}, and θ_{pmax}.

4. Results and Discussion

Figure 3 gives the overall excess air ratio versus compression ratio at different brake mean effective pressures (bmep) for the natural gas direct-injection combustion. The overall excess air ratio increases with increasing compression ratio at low and medium engine loads. However, the overall excess air ratio is increased with the increase of compression ratio up to the limit of 12 at high engine loads. The brake thermal efficiency is increased with increasing compression ratio at low and medium engine loads.[25] Thus, the engine can get the same power at an increased excess air ratio, demonstrating an increase of overall excess air ratio with increasing compression ratio. However, since an overstratified mixture is formed near the spark plug at the ignition timing when compression ratio exceeds 12 at high engine load,[25] the utilization of cylinder air is decreased at these or higher compression ratios, resulting in the decrease of brake thermal efficiency and overall excess air ratio for compression ratio larger than 12 at high engine loads.

The overall excess air ratio is larger than 1.6 when compression ratio is larger than a certain value(e.g., CR = 12) at low engine load, and this excess air ratio exceeds the lean flammability limit of the homogeneous natural gas/air mixture. This indicates that the natural gas direct-injection engine is operating under the stratified charge mode. The study also reveals that the lean burn limit of the natural gas direct-injection engine can be extended to the larger excess air ratio compared with that of a natural gas homogeneous charge engine. Since the engine operates at a large excess air ratio, the cycle-by-cycle variations of the engine become the concerned issue, and it needs to be clarified.

Pressure-Derived Combustion Parameters. Figure 4 illustrates the coefficient of variation for the indicated mean effective pressure (CoV_{pmi}) versus compressin ratio at different bmep for the natural gas direct-injection engine. The results show that CoV_{pmi} is decreased with the increase of compression ratio, and CoV_{pmi} is below 10% when compression ratio exceeds 12. This is due to increasing compression ratio will increase the cylinder gas pressure and temperature at the end of compression stroke. This will improve the growth and development of initial flame kernel and speed up the chemical reactions, resulting in an increase in burning rate and a decrease in CoV_{pmi}. In addition, increasing compression ratio will increase the ambient pressure in cylinder, which will also decrease jet penetration distance and increase jet cone angle.[40] Thus, more injected fuel will concentrate on the center part of cylinder and form a locally rich stratified mixture. This will benefit the flame development for a relatively lean mixture, increasing the combustion rate and decreasing CoV_{pmi}. Futhermore, the intensity of squish is increased with the increase of compression ratio, leading to the increase in turbulence intensity and flame propagation speed. Fast and short combustion duration is present with the increase of compression ratio, leading to the decrease in CoV_{pmi}.

However, when compression ratio is over 12, much more fuel will concentrate on the center part of cylinder in the case of high engine load, forming an overstratified mixture,[25] and

(40) Mohammadi, A.; Shioji, M.; Matsui, Y.; Kajiwara, R. *J. Eng. Gas. Turbines Power* **2008**, *130* (6), 062801.1–062801.7.

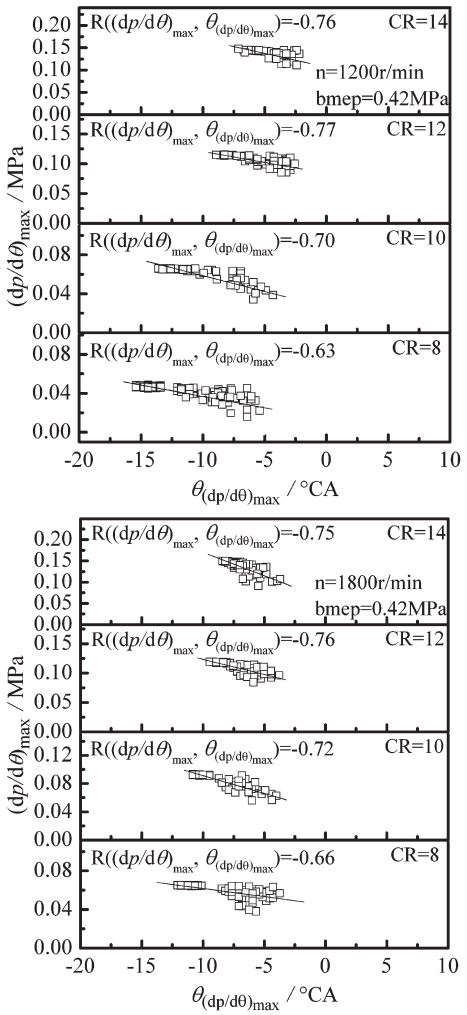

Figure 8. Interdependency between $(dp/d\theta)_{max}$ and $\theta_{(dp/d\theta)_{max}}$.

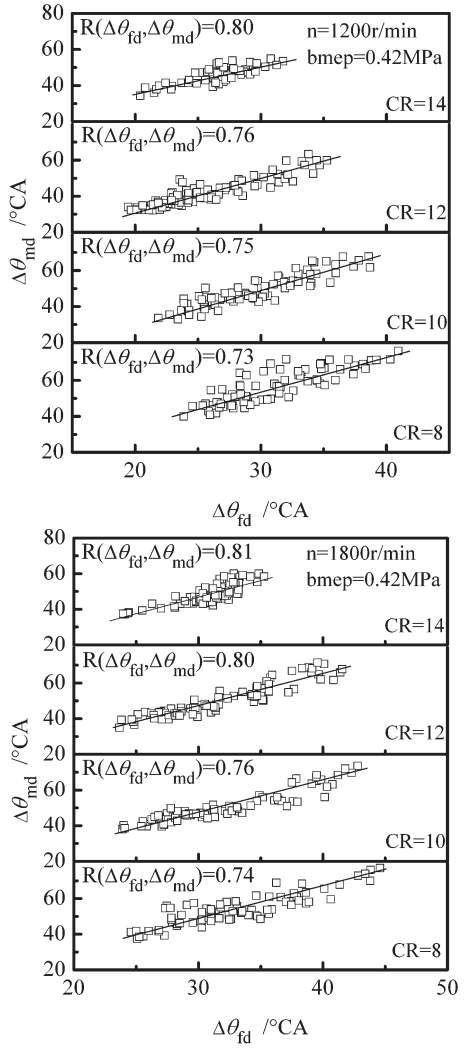

Figure 9. Interdependency between $\Delta\theta_{fd}$ and $\Delta\theta_{md}$.

the utilization of the cylinder air is decreased. This is unfavorable to mixture preparation and combustion, resulting in the decrease in combustion rate and increase in CoV_{pmi}.

For a specified compression ratio, CoV_{pmi} is decreased with the increase of engine load as shown in Figure 4. The possible reasons are that in natural gas direct-injection combustion, the overall excess air ratios are larger than 1.0 (see Figure 3) and increasing the engine load will increase the amount of fuel injected and decrease the overall excess air ratio. On one hand, the stratified mixture becomes richer with increasing engine load, increasing the burning velocity and shortening the heat release process. On the other hand, the cylinder gas temperature is increased with the increase of engine load, and this leads to an increase in flame propagation speed and a decrease in CoV_{pmi}.

The figure also shows that low cycle-by-cycle variations are present at high engine speed. At compression ratio of 12 under low engine load (bmep = 0.14 MPa), CoV_{pmi} slightly decreases from 8.30 to 7.64% as engine speed increases from 1200 to 1800 rpm. This is due to the increased turbulence intensity in cylinder at increased engine speed, leading to the increase in flame propagation speed and the decrease of cycle-by-cycle variations.

The frequency of the indicated mean effective pressure (p_{mi}) distribution at different compression ratios at bmep of 0.42 MPa is given in Figure 5. In the case of low compression ratio (CR = 8), large cycle-by-cycle variation in p_{mi} is present, demonstrating a wide range of p_{mi} distribution and a high CoV_{pmi}. The distribution of p_{mi} tends to more concentrated, and cycle-by-cycle variations decrease with the increase of compression ratio. When compression ratio is larger than 12, CoV_{pmi} is less than 10%. This is because a weakly stratified mixture is present at low compression ratio condition, and cylinder gas temperature is relatively lower at the timing of spark ignition. Also, the residual gases in the cylinder is larger at low compression ratio, increasing the residual gas fraction around the spark plug and influencing the flame kernel development. In addition, low turbulence intensity at low compression ratio leads to slow flame propagation speed and possibly bulk quenching or partial burn cycle during the flame propagation process (left side of the dashed line in Figure 5). The mean value of p_{mi} is low when partial burn cycles are present, and the occurrence of partial burn cycles will lead to the increased cycle-by-cycle variations at low compression ratio condition.

Figure 6 shows the cycle-by-cycle variations in p_{max} and p_{mi} at different compression ratios at bmep of 0.42 MPa. The average values of p_{max} and p_{mi} are plotted in bold horizontal lines. It can be seen that the standard deviation of p_{max} from its average value seems to have little difference at different

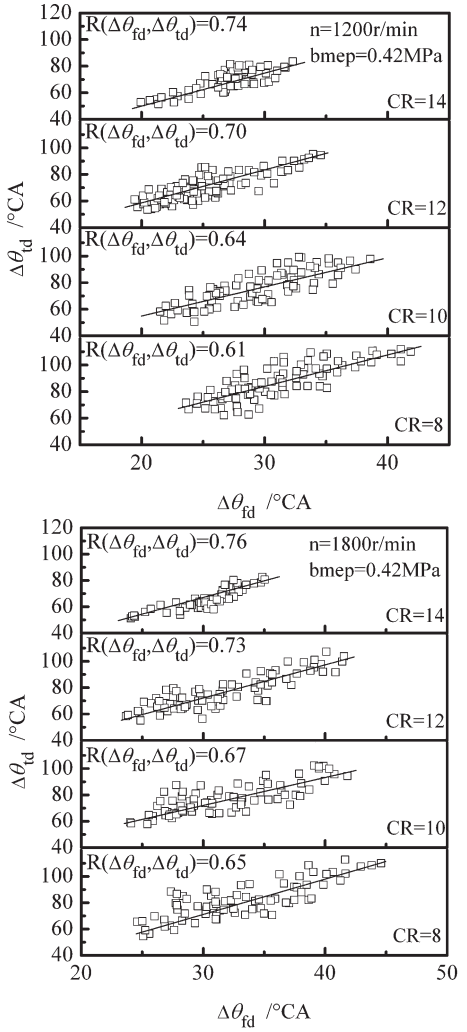

Figure 10. Interdependency between $\Delta\theta_{fd}$ and $\Delta\theta_{td}$.

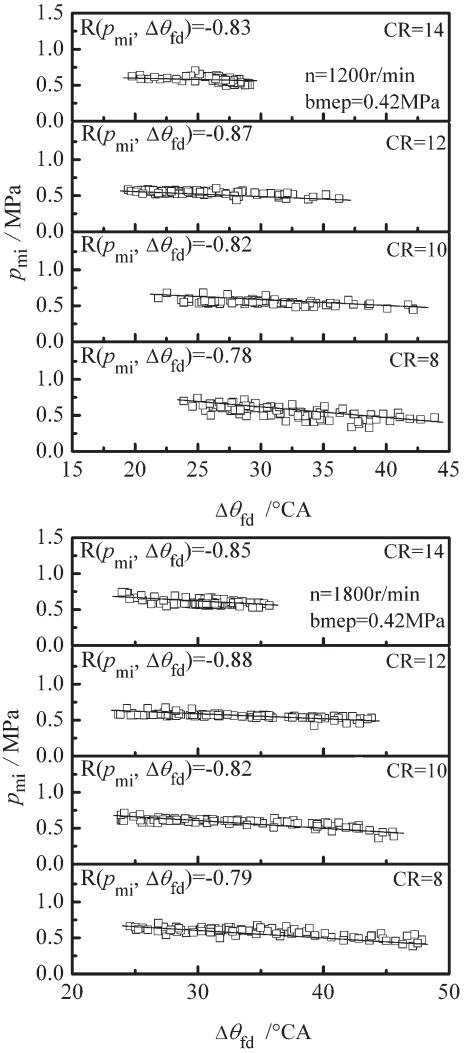

Figure 11. Interdependency between p_{mi} and $\Delta\theta_{fd}$.

compression ratios. Thus, the CoV in p_{max} (CoV_{pmax}) will be decreased with the increase of compression ratio, due to the increased average value of p_{max}, as shown in Figure 6a. However, large difference is present at the standard deviation of p_{mi} from its average value at different compression ratios. CoV_{pmi} decreases with the increase of compression ratio, and this results from the decrease of standard deviation of p_{mi} and the increase of average value of p_{mi}, as shown in Figure 6b. The study suggests that cycle-by-cycle variations can be more clearly demonstrated in CoV_{pmi} rather than in CoV_{pmax}.

Cycle-by-cycle variations of maximum cylinder pressure (p_{max}) and the corresponding crank angle of maximum cylinder pressure (θ_{pmax}) are decreased significantly with the increase of compression ratio as shown in Figure 7a. The result shows that the rate of pressure rise and the heat release rate are increased with the increase of compression ratio as cylinder temperature is increased. Better interdependence between p_{max} and θ_{pmax} is present at high compression ratios (CR $\geqslant$ 10). The cycles with high p_{max} correspond to cycles with early θ_{pmax}. In contrast to this, weak interdependence exists between p_{max} and θ_{pmax} at low compression ratio (CR = 8). Similar behavior is also presented in Figure 7b. Better interdependence exsits between p_{mi} and θ_{pmax} at high compression ratios (CR $\geqslant$ 10) while weak interdependence between p_{mi} and θ_{pmax} is present at low compression ratio (CR = 8). The occurrence of partial burn cycles may lead to weak interdependence between p_{mi} and θ_{pmax} at low compression ratio.

Cycle-by-cycle variations of maximum rate of pressure rise ($(dp/d\theta)_{max}$) and the corresponding crank angle of maximum rate of pressure rise ($\theta_{(dp/d\theta)_{max}}$) decrease significantly with the increase of compression ratio as shown in Figure 8. This would be due to the decrease of the standard deviations of $(dp/d\theta)_{max}$ and $\theta_{(dp/d\theta)_{max}}$ from their average value and the increase of the average values of $(dp/d\theta)_{max}$ and $\theta_{(dp/d\theta)_{max}}$ with the increase of compression ratio. The study indicates that fast combustion is present with the increase of compression ratio. In addition, better interdependency exists between $(dp/d\theta)_{max}$ and $\theta_{(dp/d\theta)_{max}}$ at high compression ratios (CR $\geqslant$ 10), and cycles with high values of $(dp/d\theta)_{max}$ correspond to the cycles with the advance $\theta_{(dp/d\theta)_{max}}$. This suggests that fast combustion cycles can get high pressure rise rate. At lower compression ratio (CR = 8), weak interdependence between $(dp/d\theta)_{max}$ and $\theta_{(dp/d\theta)_{max}}$ is demonstrated. This is also due to the occurrence of partial burn cycles at low compression ratio.

4.2. Combustion Duration Related Parameters. Better interdependency between flame development duration ($\Delta\theta_{fd}$) and main combustion duration ($\Delta\theta_{md}$) is present at different compression ratios as shown in Figure 9. This indicates that

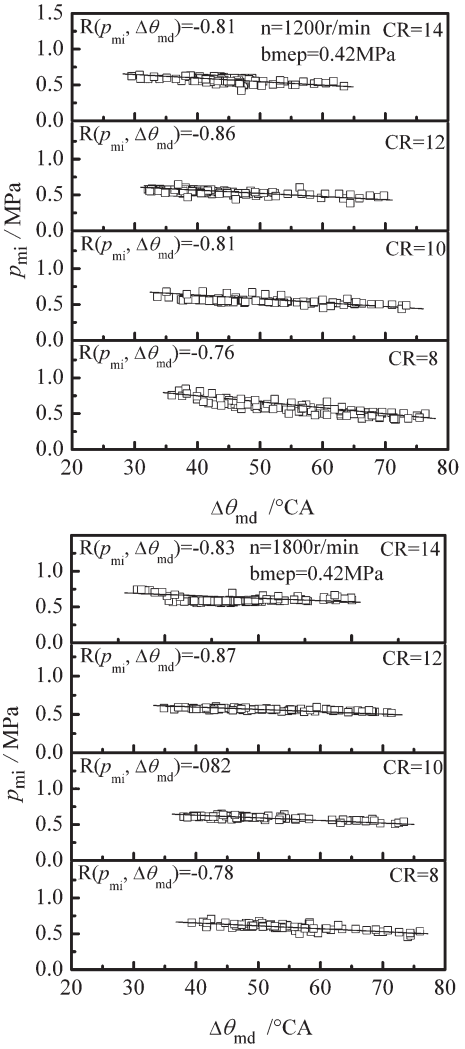

Figure 12. Interdependency between p_{mi} and $\Delta\theta_{md}$.

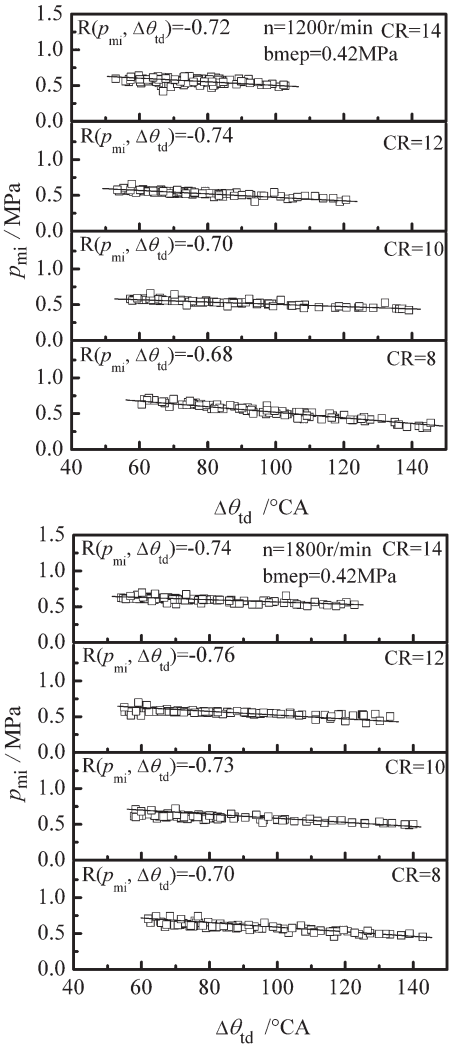

Figure 13. Interdependency between p_{mi} and $\Delta\theta_{td}$.

main combustion duration is strongly dependent on flame development duration. It reveals that small variation in flame development duration will lead to a large variation in main combustion duration, thus the cycle-by-cycle variations of the natural gas direct-injection engine may result from the variations in flame development duration.

Interdependency between flame development duration and total combustion duration at different compression ratios are illustrated in Figure 10. Although better interdependency between flame development duration and total combustion duration is present at different compression ratios, the correlation between $\Delta\theta_{fd}$ and $\Delta\theta_{td}$ is less dependent compared with that between $\Delta\theta_{fd}$ and $\Delta\theta_{md}$. This indicates that total combustion duration has weak dependence on flame development duration compared with main combustion duration.[41] The average values of $\Delta\theta_{fd}$, $\Delta\theta_{md}$, and $\Delta\theta_{td}$ decrease with the increase of compression ratio. This is the reason for decreasing cycle-by-cycle variations in the natural gas direct-injection engine.

4.3. Interdependency between Pressure-Derived and Combustion Duration Related Parameters. Figure 11 shows the interdependency between indicated mean effective pressure (p_{mi}) and flame development duration ($\Delta\theta_{fd}$) at different compression ratios. Cycle-by-cycle variations of indicated mean effective pressure and flame development duration are decreased with the increase of compression ratio. This is due to the intensity of turbulence and mixture stratification being increased with the increase of compression ratio. In addition, the cylinder gas pressure and temperature, as well as fuel concentration near the spark plug at the end of compression stroke, increase with the increase of compression ratio. Furthermore, residual gases will be decreased as compression ratio is increased. This will increase the burning rate and decrease cycle-by-cycle variations of the indicated mean effective pressure and flame development duration.

Low indicated mean effective pressure corresponds to long flame development duration. Strong interdependency between indicated mean effective pressure and flame development duration is present at different compression ratios ($R > 0.75$), as shown in Figure 11. This indicates that cyclic variations in flame development duration also determine cycle-by-cycle variations of the natural gas direct-injection engine. This is due to turbulent flow in combustion chamber; fluctuations in flow velocity and structure will result in cycle-by-cycle variations in mixture composition and distribution.[32] In addition, for the heterogeneous mixture in the cylinder of the natural gas direct-injection engine, certain fluctuation exists in the air−fuel ratio near the spark plug at

(41) Li, X. H.; Jiang, D. M.; Shen, H. X. *Chin Intern Combust Engine Eng* **1993**, *14* (04), 1–6.

the spark timing. Therefore, cycle-by-cycle variations of the engine are susceptible for the flame development duration.

Better interdependencies between the indicated mean effective pressure and main combustion duration as well as total combustion duration are present at different compression ratios in Figures 12 and 13, although the correlation coefficients between p_{mi} and $\Delta\theta_{md}$ as well as p_{mi} and $\Delta\theta_{td}$ are relatively smaller than that between p_{mi} and $\Delta\theta_{fd}$. It still gives the dependence of cycle-by-cycle variation of the indicated mean effective pressure on main combustion duration and total combustion duration in the natural gas direct-injection engine. The possible reason is that cycle-by-cycle variations of the indicated mean effective pressure is strongly correlated to cycle-by-cycle fluctuations of unburned fuel concentration at the cavity during late combustion period.[42] The cyclic variations of a natural gas direct-injection engine result from the cyclic variations in flame development duration and late combustion duration, and this is different from the homogeneous charge engine where cycle-by-cycle variations mainly result from the variations at initial stage of combustion.

5. Conclusions

Effect of compression ratio on cycle-by-cycle variations of a natural gas direct-injection engine were studied and the main results are summarized as follows: (1) Lean burn limit of the natural gas direct-injection engine is extended compared with that of a homogeneous charge nature gas engine. (2) CoV_{pmi} decreases with the increase of compression ratio, due to the effect of compression ratio on the cylinder gas pressure, temperature at the ignition timing, jet penetration distance, jet cone angle, and strength of squish in the cylinder. CoV_{pmi} tends to increase when compression ratio is larger than 12 at high load. (3) Better interdependency exists between p_{mi} and maximum cylinder pressure. Cycle-by-cycle variations can be more clearly demonstrated in CoV_{pmi} rather than in CoV_{pmax}. (4) Better interdependence exists between p_{max} and θ_{pmax}, between p_{mi} and θ_{pmax} and between $(dp/d\theta)_{max}$ and $\theta_{(dp/d\theta)_{max}}$ at high compression ratio (CR $\geqslant$ 10). Weak interdependence between p_{max} and θ_{pmax}, between p_{mi} and θ_{pmax}, and between $(dp/d\theta)_{max}$ and $\theta_{(dp/d\theta)_{max}}$ at low compression ratio (CR = 8) is present, due to occurrence of partial burn cycles at low compression ratio. (5) Better interdependence is present between flame development duration and main combustion duration, between flame development duration and total combustion duration. The average values of flame development duration, main combustion duration, and total combustion duration decrease with the increase of compression ratio. This is the reason for decreasing cycle-by-cycle variations in the natural gas direct-injection engine. (6) Better interdependence exists between the indicated mean effective pressure and flame development duration and between the indicated mean effective pressure and late combustion duration. Cyclic variations of the natural gas direct-injection engine are resulted from the cyclic variations in flame development duration and late combustion duration. This is different from homogeneous charge engine where cycle-by-cycle variations mainly result from cycle-by-cycle variations at the initial stage of combustion.

(42) Fujikawa, T.; Nomura, Y.; Hattori, Y. *Int. J. Engine Res.* **2003**, *4* (2), 143–153.

Nomenclature

ABDC = after bottom-dead-center.
ATDC = after top-dead-center.
BBDC = before bottom-dead-center.
BTDC = before top-dead-center.
bmep = brake mean effective pressure (MPa).
CoV_{pmi} = the coefficient of variation of indicated mean effective pressure.
CR = compression ratio.
$(dp/d\theta)_{max}$ = maximum rate of pressure rise with crank angle.
n_e = engine speed (rpm).
p = cylinder gas pressure (MPa).
p_{max} = maximum cylinder gas pressure (MPa).
p_{mi} = indicated mean effective pressure (MPa).
TDC = top-dead-center.
WOT = whole opening thottle.
θ = crank angle (°).
θ_{ign} = ignition advance angle (CAD BTDC).
θ_{inj} = injection advance angle (CAD BTDC).
λ = excess air ratio.
Δt_{injd} = fuel injection duration (ms).
$\Delta\theta_{fd}$ = flame development duration (CAD).
$\Delta\theta_{md}$ = main burning duration (CAD).
$\Delta\theta_{td}$ = total combustion duration(CAD).

Acknowledgment. This study is supported by the National Natural Science Foundation of China (Grant 50636040), and the National Basic Research Program of China (Grant 2007CB210006).